Electronic Supplementary Material (ESI) for Journal of Materials Chemistry A.

Supporting Information

Regulating Li-ion Flux via Engineering Oxidized ZIF-8/polyacrylonitrile Fibers Interlayer for Li Metal Battery with High Performance

Yechen Si[a], Yunhao Jiang[a], Jiayi Liu[a], Hongyu Guan[b,*], Xing-Long Wu [c], Changsheng Shan[a,*]

[a] Collaborative Innovation Center for Advanced Organic Chemical Materials Co-constructed by the Province and Ministry, Ministry of Education Key Laboratory for the Synthesis and Application of Organic Functional Molecules, College of Chemistry and Chemical Engineering, Hubei University, Wuhan 430062, PR China

[b] Center for Advanced Analytical Science, c/o School of Chemistry and Chemical Engineering, Guangzhou University, Guangzhou, Guangdong 510006, P. R. China.

[c] Department of Chemistry, Northeast Normal University, Changchun, Jilin 130024, P. R. China.

* Corresponding authors.

E-mail addresses: guanhy@gzhu.edu.cn (Hongyu Guan), csshan@hubu.edu.cn (Changsheng Shan).

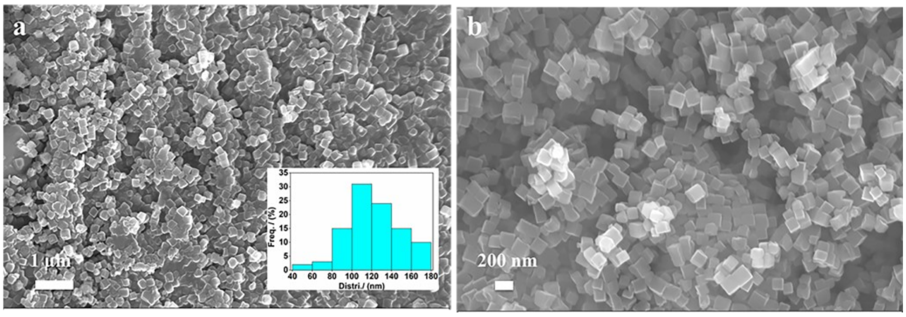

Fig. S1. SEM images and size distribution of ZIF-8.

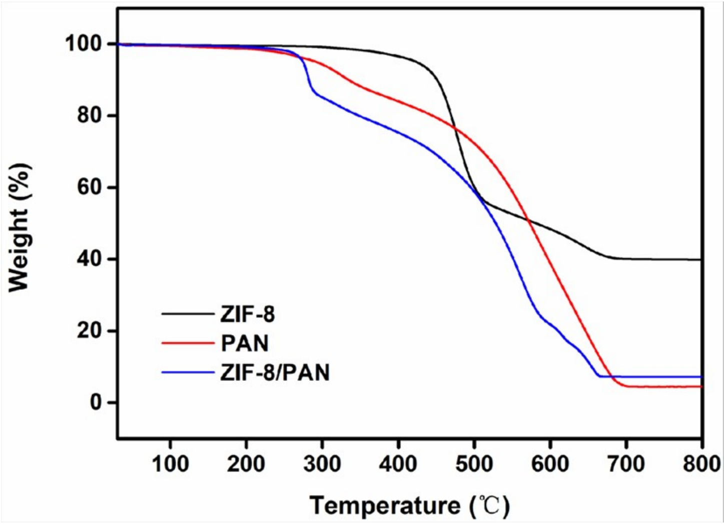

Fig. S2. The thermogravimetric curves of ZIF-8, PAN and ZIF-8/PAN under air atmosphere.

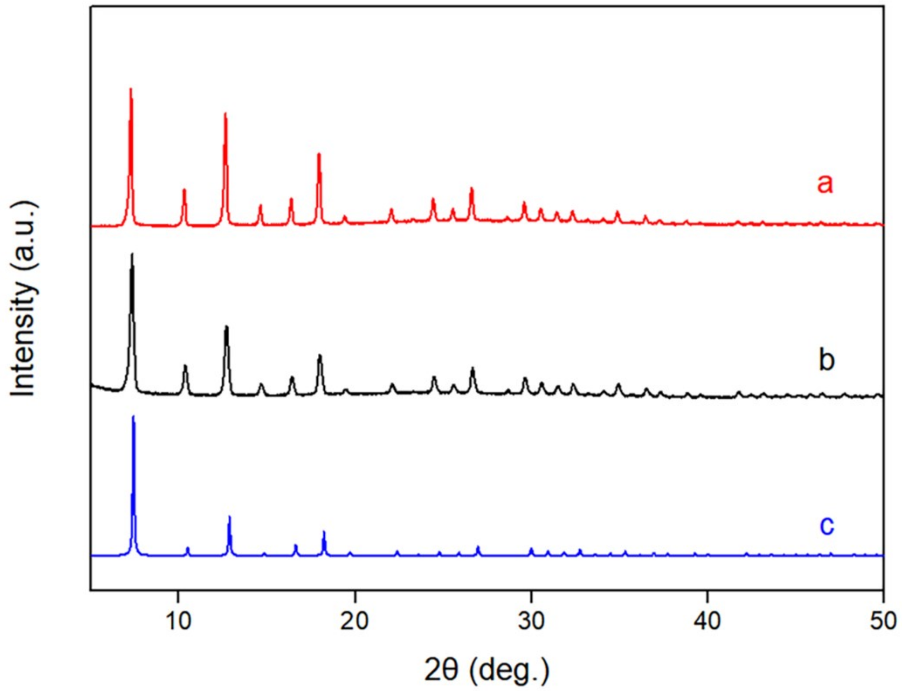

Fig. S3. XRD pattern of simulated ZIF-8 (a) and the ZIF-8 before (b) and after (c) thermal treatment.

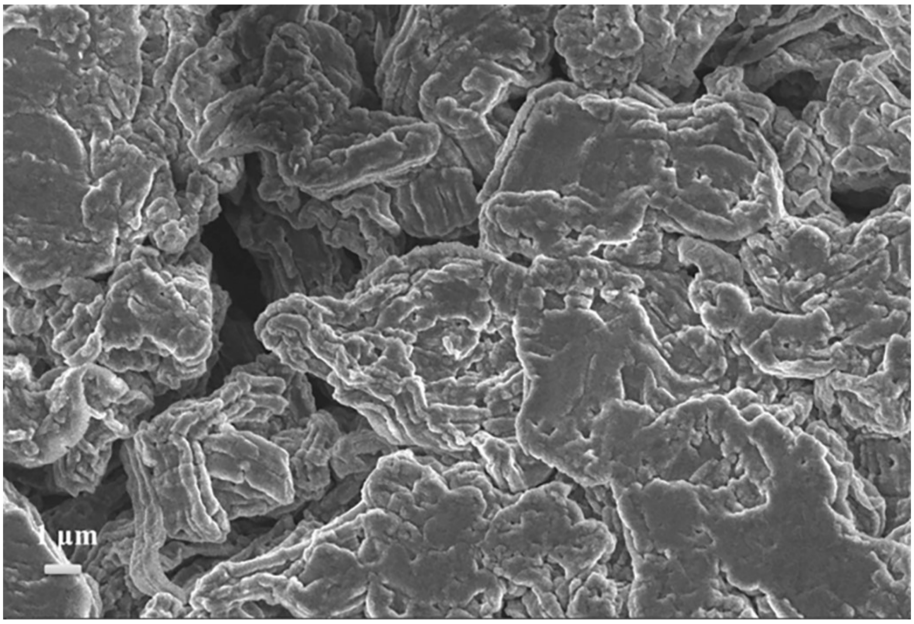

Fig. S4. SEM image of lithium metal surface without interlayer after plating 5 mAh cm^{-2} at 1 mA cm^{-2}.

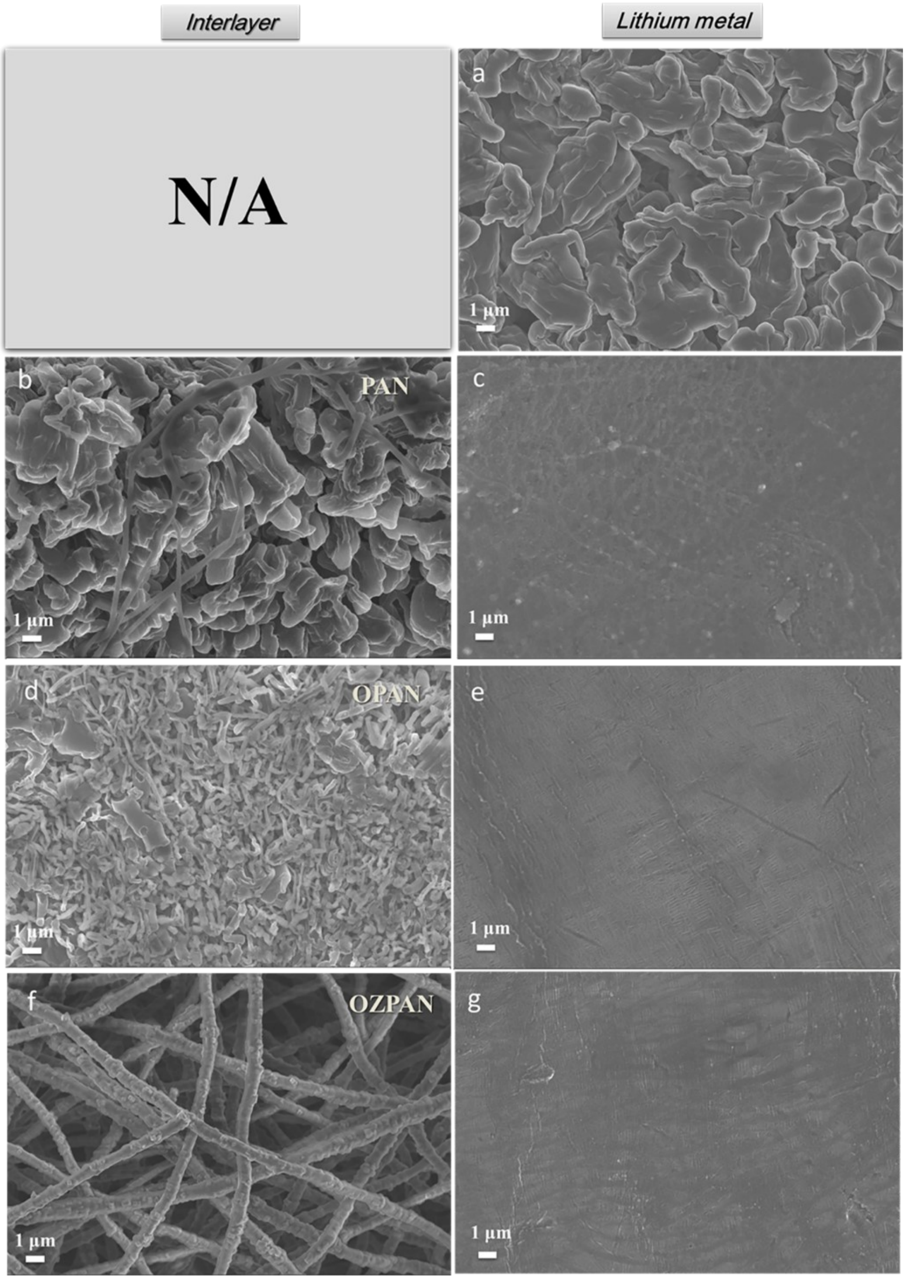

Fig. S5. (a) SEM image of lithium metal without interlayer. (b-g) SEM images of PAN (b), OPAN (d) and OZPAN (f) interlayers and corresponding lithium metal (c, e, g). Plating condition: 2 mAh cm^{-2} at 1 mA cm^{-2}.

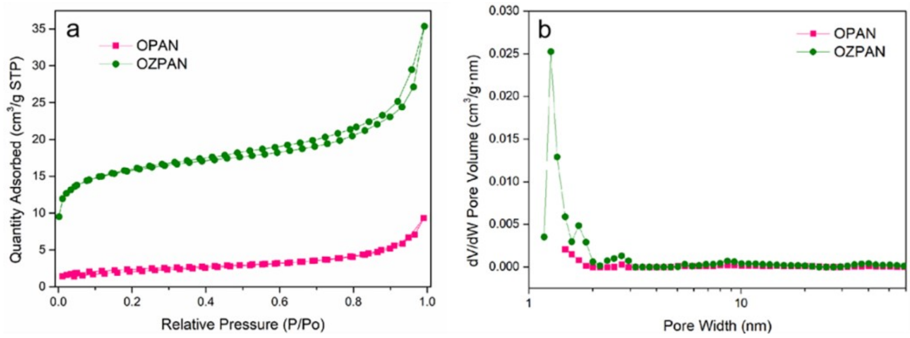

Fig. S6. Nitrogen adsorption-desorption isotherms (a) and the pore size distribution (b) of OPAN and OZPAN.

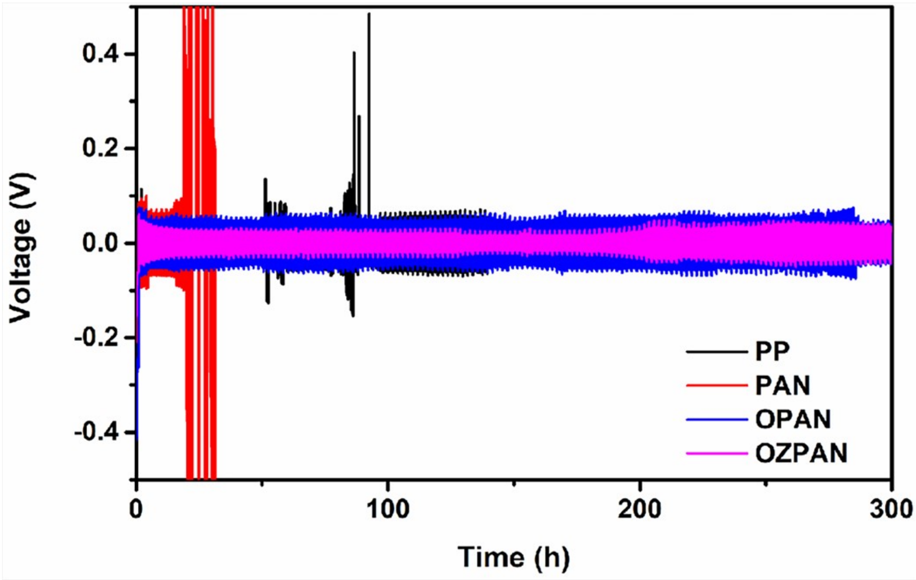

Fig. S7. Cyclic performance of Li//Li symmetric cells with PP, PAN/PP, OPAN/PP, and OZPAN/PP at a capacity of 3 mAh cm^{-2} and a current density of 3 mA cm^{-2}.

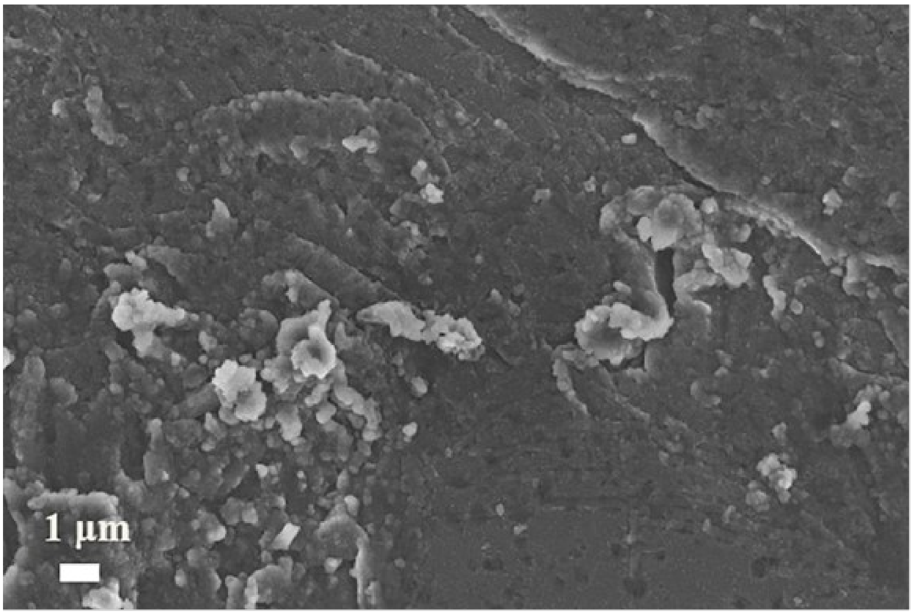

Fig. S8. The morphology of fresh lithium metal.

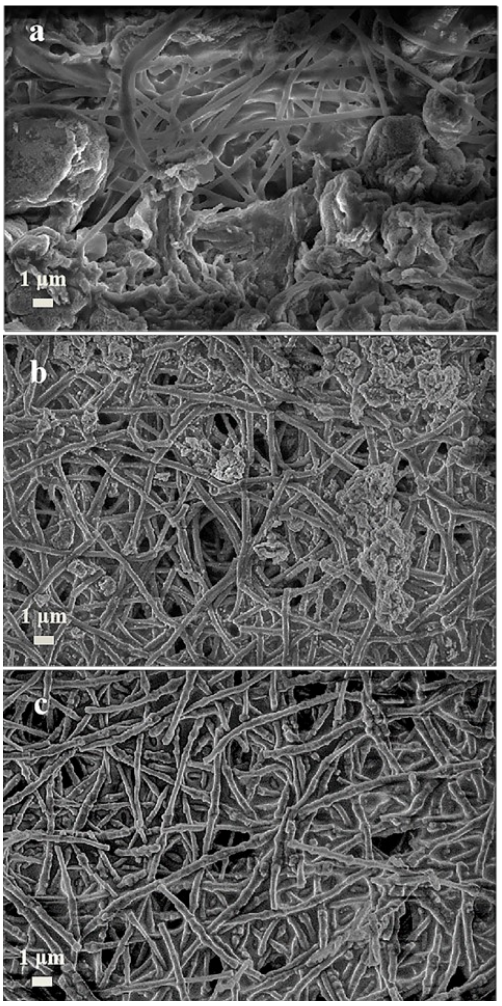

Fig. S9. The morphology structure of PAN (a), OPAN (b), and OZPAN (c) interlayers after 50 cycling.

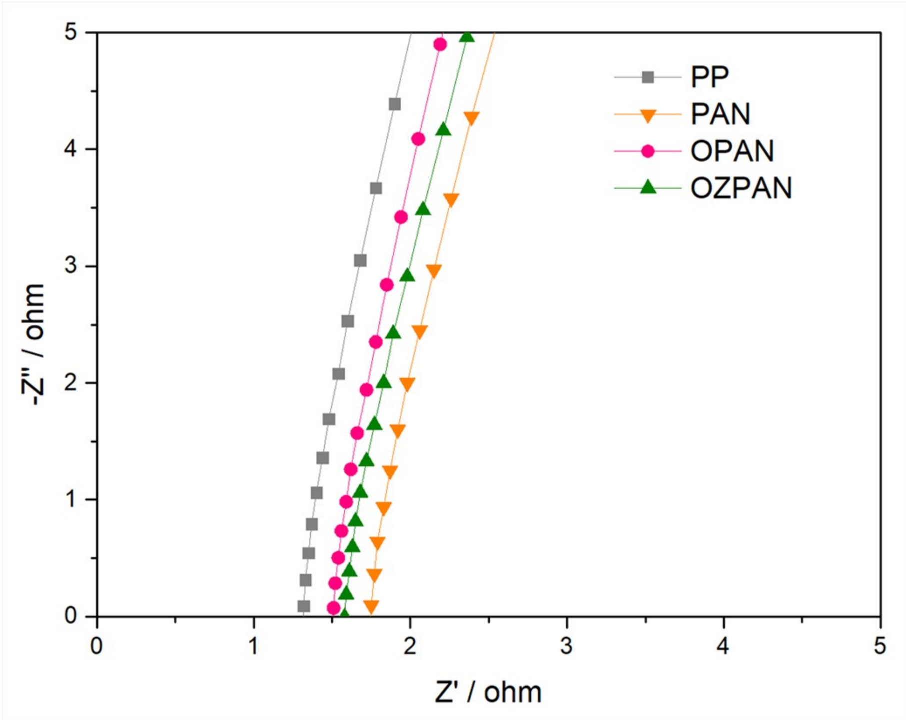

Fig. S10. Electrochemical impedance spectra of PP, PAN/PP, OPAN/PP and OZPAN/PP.

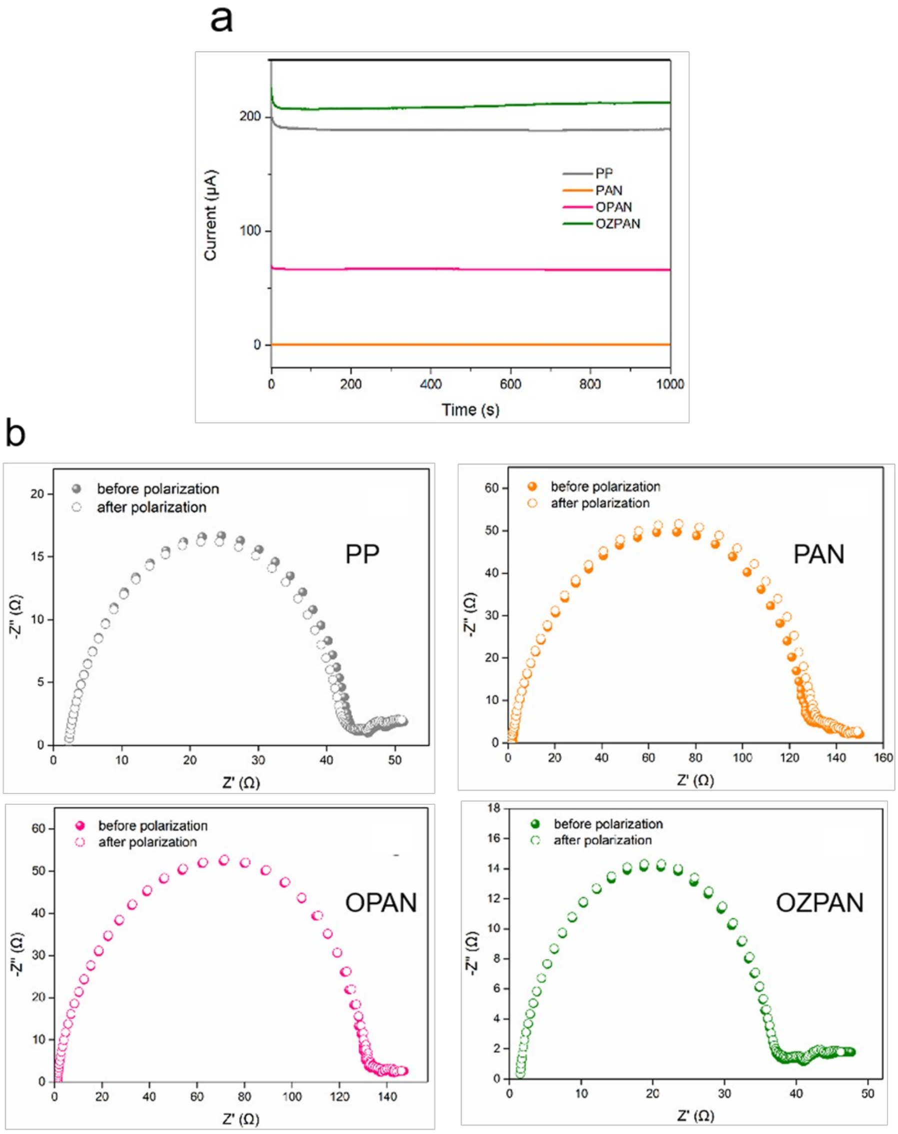

Fig. S11. (a) Chronoamperometry curves of the cells with PP, PAN/PP, OPAN/PP and OZPAN/PP. (b) The EIS for the cells with PP, PAN/PP, OPAN/PP and OZPAN/PP before and after polarization.

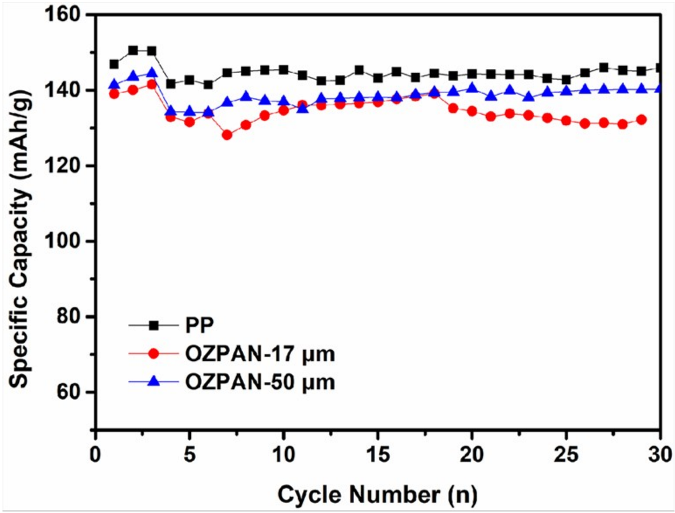

Fig. S12. The discharge capacity of Li//LFP cells at 1 C (the first 3 cycles tested at 0.5 C) without interlayer and with different thickness of OZPAN interlayer.

The effect on interlayer thickness of OZPAN fiber film has been investigated. When the thicknesses are 17 μm thin or 50 μm thick, the specific discharge capacity of Li//LFP battery with OZPAN is a little lower than that of battery without interlayer, showing poor electrochemical performance. For best battery performance shown in **Fig. 6**, the thickness of OZPAN interlayer is a range of 25 - 45 μm.

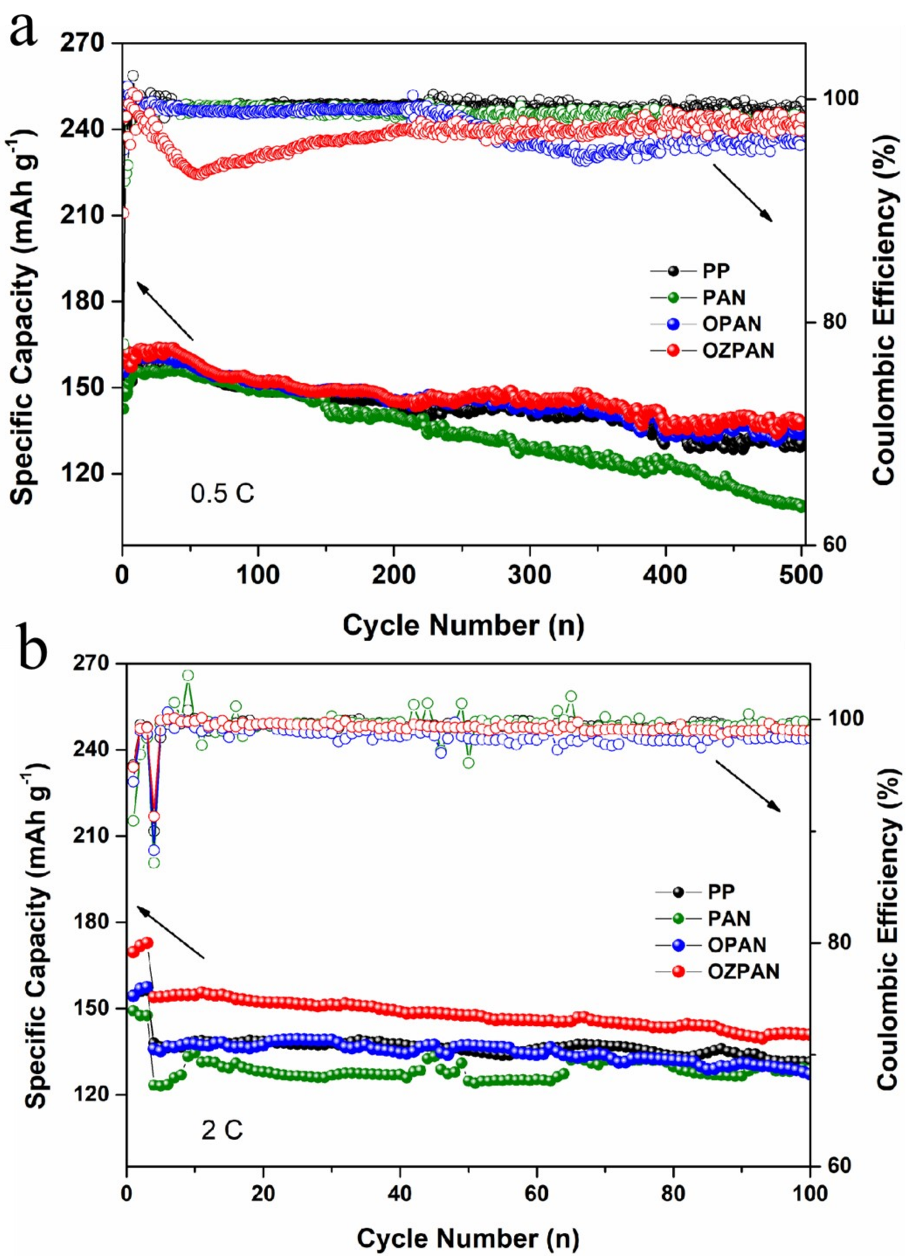

Fig. S13. Cycling stability and Coulombic efficiency of Li//LFP full cells with PP, PAN/PP, OPAN/PP and OZPAN/PP at 0.5 C (a) and 2 C (b).

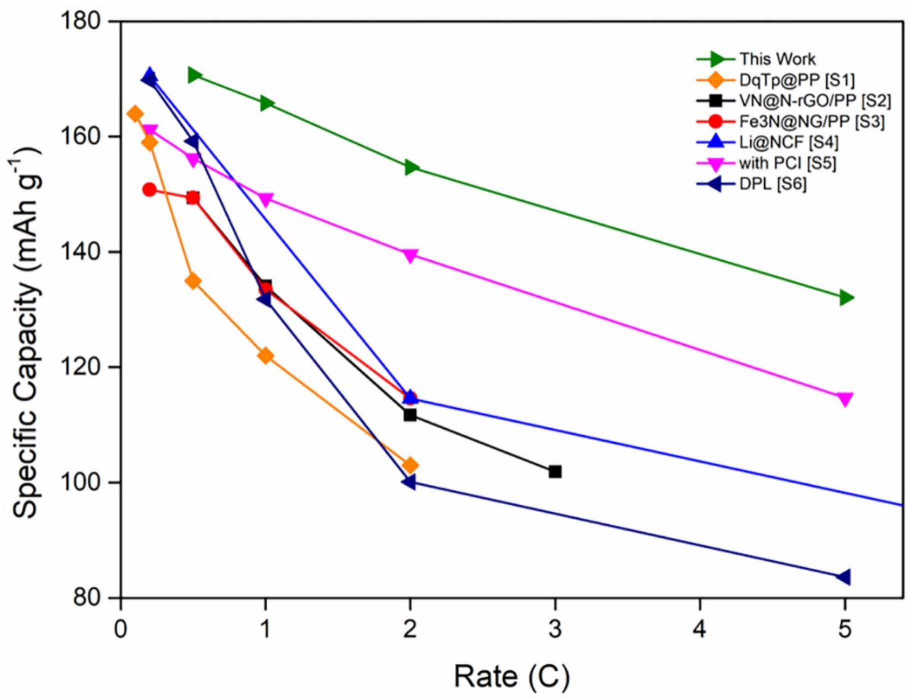

Fig. S14. Rate performance of Li//LFP cells compared to other reported works on interface engineering for lithium metal batteries.

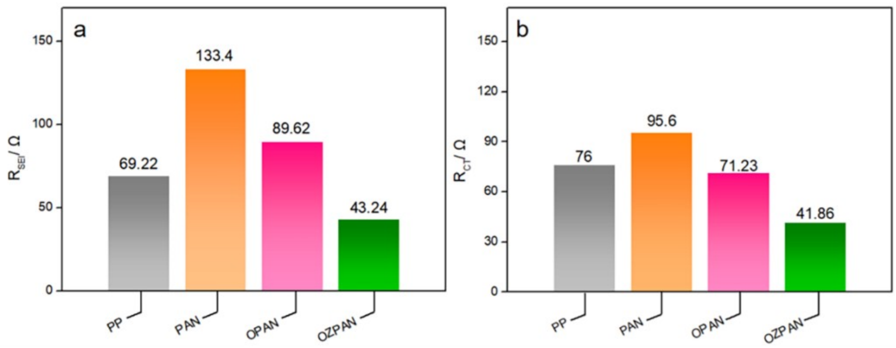

Fig. S15. Li//LFP full cells of R_{SEI} (a) and R_{CT} (b) before cycling.

Table S1. Elemental distribution of lithium metal with PP, PAN, OPAN and OZPAN by EDS.

Lithium metal (PP)		Lithium metal (PAN)		Lithium metal (OPAN)		Lithium metal (OZPAN)	
Element	Atom/%	Element	Atom/%	Element	Atom/%	Element	Atom/%
F	17.9	F	7.07	F	28.62	F	9.89
O	72.89	O	75.87	O	46.01	O	65.42
S	0.69	S	0.64	S	6.01	S	0.53
C	8.52	C	16.42	C	19.36	C	24.17

Table S2. The values of I_0 (initial current) and I_s (steady-state current) which come from Figure S11a for equation 2.

	I_0/ μA	I_s/ μA
PP	206.1	189.4
PAN/PP	0.4435	0.2442
OPAN/PP	69.71	66.14
OZPAN/PP	225.3	212.7

Table S3. Investigation of ion conductivity and Li^+ transference number.

	Ion conductivity/ mS cm^{-1}	Li^+ transference number	Reference
OZPAN/PP	2.22	0.78	This work
DpTq@PP	0.1- 0.15	0.73	[S1]
Fe_3N@NG/PP	0.70	0.54	[S3]
WNG/PP	1.140	0.5	[S7]
COF-COOH@PP	0.64	0.7	[S8]
TDAT-PE	1.127	0.375	[S9]

References

[S1] Z. Li, W. Ji, T.-X. Wang, X. Ding, B.-H. Han, W. Feng, Maximized lithiophilic carbonyl units in covalent organic frameworks as effective Li ion regulators for lithium metal batteries, Chem. Eng. J. 437 (2022) 135293. https://doi.org/10.1016/j.cej.2022.135293.

[S2] X. Zhang, Y. Chen, B. Yu, B. Wang, X. Wang, W. Zhang, D. Yang, J. He, 3D VN@ N-rGO as a Multifunctional Interlayer for Dendrite-Free and Ultrastable Lithium-Metal Batteries, ACS Appl. Mater. Interfaces 13 (2021) 20125-20136. https://doi.org/10.1021/acsami.1c02621.

[S3] X. Zhang, F. Ma, K. Srinivas, B. Yu, X. Chen, B. Wang, X. Wang, D. Liu, Z. Zhang, J. He, Fe3N@ N-doped graphene as a lithiophilic interlayer for highly stable lithium metal batteries, Energy Stor. Mater. 45 (2022) 656-666. https://doi.org/10.1016/j.ensm.2021.12.010.

[S4] J. Man, K. Liu, H. Zhang, Y. Du, J. Yin, X. Wang, J. Sun, Dendrite-free lithium metal anode enabled by ion/electron-conductive N-doped 3D carbon fiber interlayer, J. Power Sources 489 (2021) 229524. https://doi.org/10.1016/j.jpowsour.2021.229524.

[S5] H. Liu, D. Peng, T. Xu, K. Cai, K. Sun, Z. Wang, Porous conductive interlayer for dendrite-free lithium metal battery, J. Energy Chem. 53 (2021) 412-418. https://doi.org/10.1016/j.jechem.2020.07.030.

[S6] K. Zhang, F. Wu, K. Zhang, S. Weng, X. Wang, M. Gao, Y. Sun, D. Cao, Y. Bai, H. Xu, Chlorinated dual-protective layers as interfacial stabilizer for dendrite-free lithium metal anode, Energy Stor. Mater. 41 (2021), 485-494. https://doi.org/10.1016/j.ensm.2021.06.023.

[S7] X. Zhang, Y. Chen, F. Ma, X. Chen, B. Wang, Q. Wu, Z. Zhang, D. Liu, W. Zhang, J. He, Regulating Li uniform deposition by lithiophilic interlayer as Li-ion redistributor for highly stable lithium metal batteries, *Chem. Eng. J.* 436 (2022) 134945. https://doi.org/10.1016/j.cej.2022.134945.

[S8] Q. An, H.e. Wang, G. Zhao, S. Wang, L. Xu, H. Wang, Y. Fu, H. Guo, Understanding Dual-Polar Group Functionalized COFs for Accelerating Li-Ion Transport and Dendrite-Free Deposition in Lithium Metal Anodes, Energy Environ. Mater. 0 (2022) 1-10. https://doi.org/10.1002/eem2.12345.

[S9] J. Yang, L. Xu, S. Li, C. Peng, The role of titanium-deficient anatase TiO2 interlayers in boosting lithium–sulfur battery performance: polysulfide trapping, catalysis and enhanced lithium ion transport, Nanoscale 12 (2020) 4645-4654. https://doi.org/10.1039/C9NR10349J.